14th IEA Heat Pump Conference
15-18 May 2023, Chicago, Illinois

Maximizing operational efficiency of heat pumps with Model Predictive Control: An experimental case study for residential application

Stephan Göbel[a,*], Phillip Stoffel[a], Florian Will[a], Christian Vering[a], Dirk Müller[a]

[a] RWTH Aachen University, Institute for Energy Efficient Buildings and Indoor Climate, Aachen, Germany
[*]Corresponding author

Abstract

In residential heating applications, electrically-driven heat pump systems enable the integration of renewable energy sources (RES) and, thus, systematic sector defossilation. Since the heating demand of buildings and RES availability are time-variant and time-shifted, it is challenging to ensure optimal heat pump system operation. Optimal heat pump system operation requires access to reliable system interfaces and consistent use of higher control strategies such as model predictive control (MPC). However, missing interfaces prevent the spread of MPC in the field and call for conventional controls such as heating curves reducing the overall potential.
This work shows the potential of MPC for heat pump systems by exploiting system interfaces in an experimental case study. We use a heat pump test bench coupled to a dynamic building performance simulation model in the hardware-in-the-loop approach and investigate two control levels: The refrigerant cycle controller ensures stable superheat and resilient operation; the system controller minimizes the heat pump power consumption within the comfort constraints. We analyze two MPC interfaces to control the system: First, the MPC sets the flow temperature, while a PID controls the compressor speed. Second, the MPC directly adjusts the compressor speed. We compare both MPC strategies with a conventional heating curve controller.
The results highlight the need for heat pump interfaces to widespread MPC. Both MPC strategies reduce the heat pump power consumption by up to 20.25 %. Adjusting the flow temperature by MPC results in the lowest energy consumption but many compressor starts and comfort losses. Direct compressor-controlled systems claim the best results concerning comfort constraints and lead to a resilient operation by reducing on-off behavior.

Selection and/or peer-review under the responsibility of the organizers of the 14th IEA Heat Pump Conference 2023.

Keywords: system control; hardware-in-the-loop; experiment; simulation; underfloor heating; building performance simulation

1. Introduction

For all sectors, the IPC report shows the need for consistent defossilation to meet climate goals and mitigate climate impact consequences [1]. In particular, the building sector is responsible for up to 30 % of total energy consumption [2]. While, in other sectors, standardized solutions already exist to reduce emissions on a larger scale, there are still major challenges in the building sector due to the high degree of individuality of buildings and occupants [3]. Solving one challenge to reduce the emissions related to heating purposes, heat pump systems can exchange conventional combustion-based heating systems. Electrically-driven heat pump systems are the most efficient solution for defossilation the building sector, as they can provide CO_2-neutral heat when using electricity from renewable energy sources (RES). However, optimal heat pump integration and operation lead to complex system setups and controls since the heating demand and renewable energy sources (RES) availability are time-variant and time-shifted. To capture time-variance and time-shifting, model predictive

* Corresponding author
E-mail address: stephan.goebel@eonerc.rwth-aachen.de

control (MPC) applications are a potential solution in the recent literature. MPC strategies reduce energy consumption by 13 % to 28 %, depending on the heat pump system setup [4]. However, most heat pump systems in the field operate in weather compensation mode using an outdoor temperature-dependent supply temperature (heating curve). As a result, heat pump systems are often not operated optimally, considerably reducing their potential in many cases.

To optimally operate heat pump systems and fully exploit the potential of MPC, there is the need to identify barriers preventing the transfer into practice. In the literature, there are multiple reasons for the slow implementation of MPC approaches in the building sector. First, the development of MPC in building energy systems (BES) needs deep expert knowledge and high hardware and software requirements [5]. Second, individual buildings require individual process models for the controller configuration and, thus, increase the development time [6]. In a recent theoretical study, Stoffel et al. show a data-driven MPC using black-box models (BBMPC) that perform similarly to detailed white-box MPC approaches [7]. In addition, online learning offers continuous improvement of the BBMPC process models reducing the gap compared to more development-intensive MPC approaches. While Stoffel et al. follow a theoretical approach where almost all interfaces can be made available, in practice, interfaces may not be available for safety reasons or the manufacturer's market strategy.

Today, the available interfaces to control heat pumps are very limited, preventing the optimal operation of heat pump systems. In the case of market-available heat pumps, a potential MPC can only control a manipulated variable via the SmartGrid Ready interface that indirectly controls a system variable (e.g., flow temperature). Typically, an internal heat pump controller (usually conventional PID-Controller) still adjusts the control variables of the heat pump (e.g., compressor speed) regardless of whether this is purposeful for the overall system. Hence, the literature shows only studies in which the MPC cannot directly control the compressor speed, which makes the internal controller the limiting factor for optimal system operation [8]. However, to the best of the author's knowledge, such limiting factors are not discussed in the literature.

In the literature, studies show high potential for MPC in BES based on numerical approaches and neglect limiting factors of real-world operation. In addition, many approaches use simplified black-box models or linearized models to predict the heat pump's behavior. However, the heat pump is a closed thermodynamic cycle inherently covering nonlinear dependencies between state and control variables. Considering the complex thermodynamic relationships leads to a complex and computationally intensive model that is often avoided in MPC approaches to solve the underlying optimization problem in a reasonable time. This paper closes the identified research gaps and proves the proposed method in a simulative and experimental case study:

- To reduce expert knowledge for setting up process models, we use data-driven models to minimize the modeling effort.
- To prove consistent thermodynamics and prediction accuracy, we conduct measurement campaigns that substantiate our approaches.
- To avoid manufacturer-related interface limitations, we use a fully controllable heat pump test bench with all relevant interfaces [9].
- To prove the proposed method under realistic, dynamic, and repeatable boundary conditions, we use the hardware-in-the-loop approach by coupling a heat pump test bench to a virtual building.

The paper is structured as follows:

- Section 2 describes the experimental setup and the controller's structure.
- Section 3 shows the results of the simulative and experimental case studies.
- Section 4 discusses the results and underlines the potential of the proposed method.
- Section 5 concludes all findings and gives recommendations for future work.

2. Method: MPC for heat pump systems

The proposed method of this work integrates an MPC system controller into a heat pump test bench., This work uses the experimental hardware-in-the-loop (HiL) approach to assess the potential of MPC compared to conventional controllers under dynamic, realistic, and repeatable boundary conditions. This approach couples real hardware with simulation models that lead to dynamic and realistic environments. This section describes the HiL setup and explains the developed system controller. Furthermore, we introduce the performed case studies and define the used key performance indicators (KPI).

2.1. Experimental Setup

This section presents the HiL approach for the experimental case study. HiL connects virtual buildings with real heat generators. In this work, we focus on the behavior of the heat pump and the potential of the MPC system controller. Figure 1 shows a schematical overview of the implemented HiL framework.

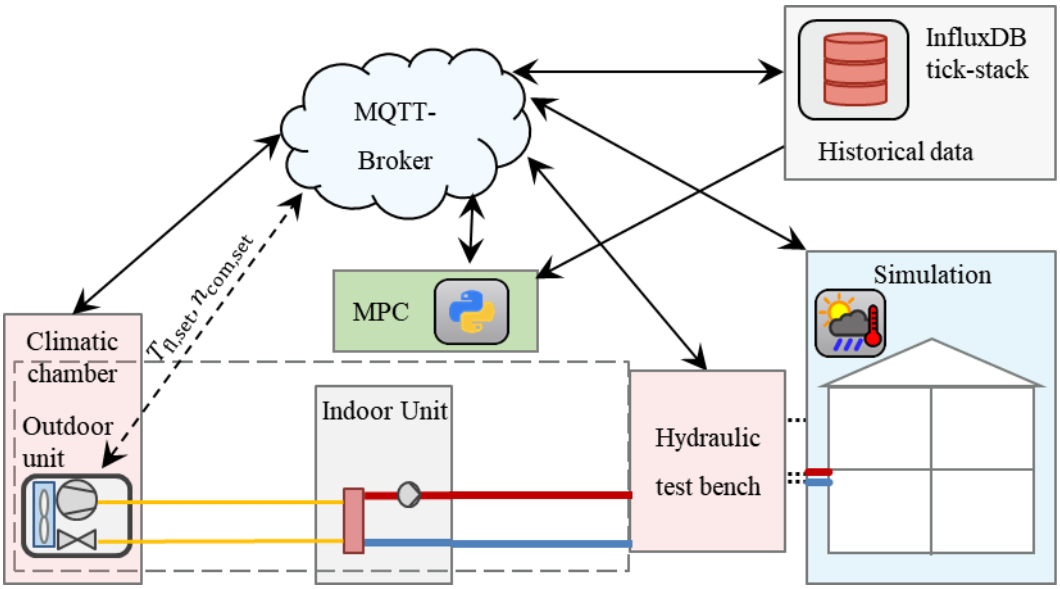

Figure 1: Schematic overview of HiL setup: heat pump test bench (indoor unit and outdoor unit), Climatic chamber, Hydraulic test bench, simulation model, MPC system controller, InfluxDB tick-stack, and MQTT Broker

The system consists of an air-to-water heat pump in split design, test benches (climatic chamber and hydraulic test bench), a building performance simulation model, the cloud-based data infrastructure (MQTT-Broker and InfluxDB tick-stack), and the MPC system controller. The several components are described in the following:

Air-to-water heat pump:

In this work, we use a self-developed air-to-water heat pump with a nominal heating capacity of 7 kW in operating point A7W35 (ambient temperature: 7 °C, supply temperature: 35 °C). We built the heat pump in split design: the outdoor unit (OU) consists of the compressor, evaporator, and expansion valve; the indoor unit (IU) consists of a condenser and a water pump for the hydraulic cycle.

The heat pump uses an inverter-driven scroll compressor operating between 30 Hz and 90 Hz, indicating a possible part load operation of 1/3 of the full load. Using a PLC and measuring terminals, all sensor data are collected, and all set values are written. In previous work, we developed control strategies for a safe and efficient operation regarding superheat control [9]. Thus, the internal heat pump controller controls two subsystems (see Figure 2 and Figure 3).

First, the superheat control (Figure 2) regulates the expansion valve and ensures that gaseous refrigerant enters the compressor's inlet. The detailed controller development is described in Göbel et al. [9].

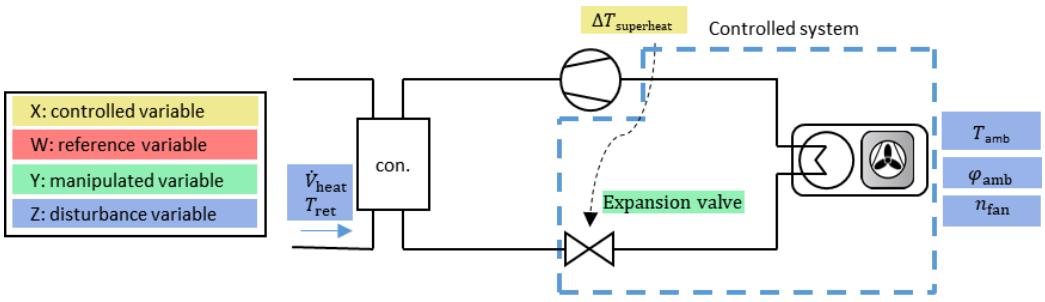

Figure 2: Superheat control of the A/W heat pump

According to Figure 3, the flow temperature T_{fl} can be controlled by manipulating the compressor speed n_{com}. In the market-available heat pumps, an internal PID controller is used to adjust the control variable. However, this controller has no direct interface for MPC applications. In this work, we open this controller interface to manipulate the compressor speed $n_{\mathrm{com,set}}$ directly by the system controller. Within the HiL approach, the air-to-water heat pump is coupled to a virtual building, which is explained in the following.

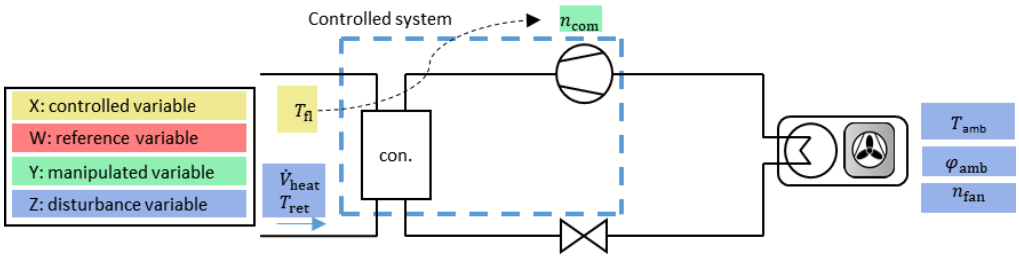

Figure 3: Flow temperature control of the A/W heat pump

Building performance simulation model

We calculate the building performance simulation for the HiL framework using the BESMod Modelica library [10]. In this context, we integrate MQTT communication blocks into the hydraulic subsystem. A single-zone Modelica building performance simulation model calculates the thermal behavior of a building. The air temperature of the single zone represents the room temperature, which is the controlled variable. The model's parameters are obtained from TEASER [11]. The building envelope covers a net floor area of 130 m^2. Following DIN EN 12831, the resulting heat load at -12 °C is 6.596 W. We implement an underfloor heating system model to transfer heat from the hydraulic cycle to the building envelope. The total activated floor's capacity is $52.629\ \mathrm{kJ\ K^{-1}}$ which is equal to a water volume of $12.59\ \mathrm{m^3}$. Due to this high capacity, we avoid an additional buffer tank within the hydraulic system. To connect the described simulation model to the heat pump, we use test benches, which are explained in the following section.

Test benches

The air-to-water heat pump is located in a climatic chamber that emulates dynamic ambient conditions. The climatic chamber captures ambient conditions between -20 °C and 40 °C and humidity up to 100 %. For this purpose, the climatic chamber has an air handling unit with heat exchangers for cooling and dehumidification, an electric heating coil, and an isothermic steam humidifier. The hydraulic test bench controls the return flow temperature and the volume flow of the heating cycle, which the dynamic building performance simulation model calculates. The return temperature is adjusted using a three-way mixing valve, ensuring fast responses and low delay times due to mixing. While the test benches are the physical connection between the simulation model and the heat pump, the cloud-based data infrastructure is the digital connection between all components.

Cloud-based data infrastructure

All components (simulation models, test benches, system controller) communicate with the overall MQTT broker to which they can send data and subscribe to topics. The task of the MQTT broker is to distribute the data. Each component subscribes to the necessary topics. When the broker receives messages for corresponding topics, it is passed on to the corresponding component. The components send their data with a time increment of one second. The communication latency is in the range of milliseconds, allowing the components receive the subscribed messages in the proposed time increment. While the time constants of thermal systems with high capacity (as shown above) are significantly higher than the time increment and the latency, the frequency, and the latency do not affect the system's interaction.

Completing the communication infrastructure, we use the InfluxDB tick-stack to store and visualize all time-varying data, which is communicated via the MQTT broker [12], [13]. Since no historical data is available via the MQTT broker, the system controller requests this data directly from the InfluxDB time series database using HTTP. In this work, we integrate the system controller into the described framework, which we explain in more detail below.

System Controller

The controller needs access to the MQTT brokers and the InfluxDB tick-stack. In this framework, the MPC can run on any server in a cloud system. In this work, the system controller is the device under test, exploiting MPC's potential using different interfaces compared to conventional heating curves. Section 2.2 describes the controller in detail.

2.2. Data-driven model predictive control

The developed MPC maintains thermal comfort by keeping the zone's air temperature within the comfort constraints and simultaneously minimizes the heat pump's power consumption. The cost function of the resulting optimal control problem (OCP) (1) – (7) is given in (1). We penalize the violation ϵ of comfort constraints (4) with $C_1 = 10$. Furthermore, we consider energy consumption by minimizing the control input u. Depending on the experiment, the control input u can either be the actual heat pump modulation (compressor speed) ($C_{2,n_{\mathrm{com}}} = 0.1$) or the flow temperature of the heat pump ($C_{2,t_{\mathrm{flow}}} = 0.1 \cdot 1/300$). The weight $C_{2,t_{\mathrm{flow}}}$ is scaled with 1/300 because the absolute values of the flow temperature are higher than the ones of the heat pump modulation. The third term $C_3 \Delta u_k^2$ ($C_{3,t_{\mathrm{flow}}} = 0.005 \cdot 1/30$) ; $C_{3,n_{\mathrm{com}}} = 0.1$) describes the cost of changing the manipulated variable, which prevents the system from oscillating. The term is squared so that both negative and positive changes are considered. We determine the values of all weights C heuristically. In future work, we also plan to model and minimize the heat pump's electric power.

$$\min_{u,\epsilon} \sum_{k=0}^{N} C_1 \epsilon_k^2 + C_2 u_k + C_3 \Delta u_k^2 \tag{1}$$

$$\text{s.t. } \Delta T_{air,k} = f_{ann}(T_{air,k}, \dots, T_{air,k-m_T}, u_k, \dots, u_{k-m_u}, d_k, \dots, d_{k-m_d}) \tag{2}$$

$$T_{air,k+1} = \Delta T_{air,k} + T_{air,k} \tag{3}$$

$$T_{air,min,k} - \epsilon_k \leq T_{air,k} \leq T_{air,max,k} + \epsilon \tag{4}$$

$$0 \leq \epsilon \tag{5}$$

$$u_{min} \leq u_k \leq u_{max} \tag{6}$$

$$\forall k \in [0, \dots, N-1] \tag{7}$$

Crucial for the successful implementation of MPC is the underlying process model to predict the building's and heat pump's behavior (2) – (3). In this case, we use an artificial neural network (ANN) to predict the zone's temperature with all inherent system dynamics. To predict the temperature change ΔT_{air} during time step k, we consider the last m_T temperatures, the last m_u controls, and the last m_d measured disturbances d (solar radiation and ambient temperature). Thus, we use a nonlinear, autoregressive process model with exogenous inputs (NARX). Using this process model leads to a nonlinear optimization problem, which we solve efficiently using Casadi and Ipopt [14], [15]. Details on the integration of ANNs as process models in an MPC can be found in previous works of the authors [7], [15]–[17]. The OCP's prediction horizon N is 36 with a time step size of 10 min, which results in a prediction of 6 hours.

Safe operation of the MPC requires validity of the underlying process model in the whole operation range. For that reason, we pre-train the ANN with simulation data. The system identification of the simulation model is performed by choosing temperature setpoints according to a square curve for a baseline PID controller for two weeks each in winter, spring, and fall from a test reference year [18]. Here, the data set is split into 80% training, 10% validation, and 10% testing

Besides the training data for setting up a reasonable process model using ANNs, the hyperparameter tuning of ANNs is crucial. Tuneable hyperparameters are the number of layers, the number of neurons in each layer, and the activation function. In this work, a brute-force hyperparameter optimization is performed. For this reason, several ANNs with different architectures are trained and evaluated on the test set. The ANNs with the

highest accuracy are finally used as a process model in the MPC. A batch normalizing layer serves as the input layer since it efficiently scales the features, stabilizes, and speeds up the training process [19]. The output layer uses a linear activation function. We constrain the hyperparameter optimization to use relatively small ANNs with one or two hidden layers and 4 to 32 neurons to compute the optimization problem more efficiently and reduce the risk of overfitting. After hyperparameter tuning, the final ANN has one hidden layer with 16 neurons. The activation function for the hidden layer's neurons is the softsign function. We analyze and benchmark the developed system controller in a case study described below.

2.3. Case Study

In this work, we integrate MPC into a heat pump system controller and investigate the impact of the interface between the system controller and the heat pump system on the overall performance of a building energy system.

For this purpose, we consider two interfaces and a benchmark control:

1. **Benchmark control: Heating curve:**
   The used benchmark control is a weather compensation heating curve which takes the nominal flow temperature $T_{\mathrm{fl,nom}}$, the current room set temperature $T_{\mathrm{room,set}}$, the ambient temperature T_{amb} and the nominal ambient temperature $T_{\mathrm{amb,nom}}$ into account to calculate the set flow temperature $T_{\mathrm{fl,set}}$ for the heat pump. Equation 8 shows the correlation between the variables.

$$T_{fl,set} = \left(T_{fl,nom} - T_{room,set}\right) \cdot \left(\frac{T_{room,set} - T_{amb}}{T_{room,set} - T_{amb,nom}}\right)^{\frac{1}{n}} + T_{room,set} \tag{8}$$

   The parameter *n* describes the heat curve's gradient and is constant at 1.2. The equation results in the nominal flow temperature at the nominal ambient temperature. Because the equation considers the current room set temperature, the set flow temperature is decreased during periods of low room set temperatures. Besides the flow temperature control, a valve manipulates the volume flow into the underfloor heating to further control the room temperature resulting in a dynamic volume flow.
2. **Manipulated variable: Flow temperature**:
   The MPC controls the room temperature by manipulating the flow temperature of the heat pump. The internal controller of the heat pump regulates the supply temperature with the help of the compressor speed. Furthermore, the internal controller considers the heat pump's physical constraints (e.g., min compressor speed = 30 Hz). The volume flow is constant at the nominal flow.
3. **Manipulated variable: Compressor speed**
   The MPC controls the room temperature by manipulating the compressor speed. The heat pump's internal control only interacts with security issues. The MPC knows the heat pump's constraints. Since the manipulated variable has a discontinuous step between 0 and 30 Hz, the heat pump gets turned on above 30 Hz. Below a compressor speed of 30 Hz, the compressor does not operate. The volume flow is constant at the nominal flow.

Figure 4 shows the reference variable for the heating curve and the comfort band for evaluating the room temperature. The approaches with MPC use the band directly as a reference variable. For the heating curve, we shift the reference variable so that the room temperature corresponds approximately to the room setpoint temperature at the beginning of the comfort phase (interval of the higher room setpoint temperature).

We use weather data for the location of Potsdam as a boundary condition of the energy system [18]. We determine reference days with the help of sensitivity analysis and clustering [20]. This work only considers this system's winter reference day, Jan. 11. The day has a mean temperature of 1.32 °C, representing 114 days in the year in Potsdam.

We perform a simulative and experimental case study for this work. The simulative study consists of three cases. The study considers the system with the heating curve controller, the MPC manipulating the flow temperature, and the MPC using the compressor speed as the manipulated variable. We only consider the two MPC controllers for the experimental study without an additional benchmark test since we focus on the interface itself.

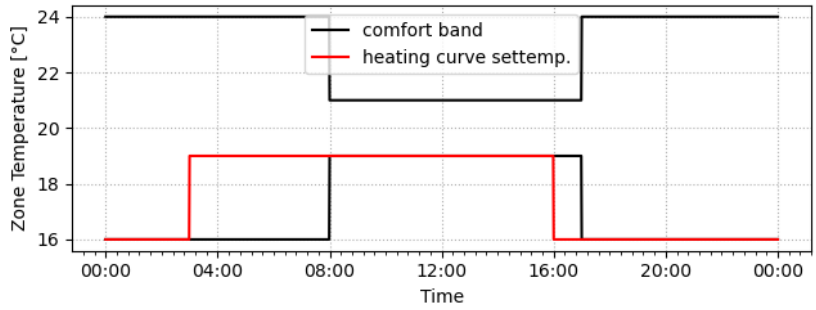

Figure 4: Comfort band for MPC and room setpoint for heating curve for a complete day

2.4. KPI Definition

We evaluate our results with different KPI definitions, which we explain in the following section:

Discomfort:

All building energy systems have a trade-off between discomfort and energy consumption. In our work, we calculate the total discomfort as follows:

$$\int_{t=0}^{t_{end}} |T_{room} - T_{room,set}| \; dt \tag{9}$$

Energy Consumption:

We consider for the energy consumption, the total electrical energy consumption of the heat pump:

$$W_{el,hp} = \int_{t=0}^{t_{end}} P_{el} \; dt \tag{10}$$

Seasonal Coefficient of Performance (SCOP):

To evaluate the heat pump's efficiency, we use the integrated COP of the heat pump over the day considered. To do so, we integrate the provided heat flow into the building $\dot{Q}_{sh}$.

$$SCOP = \frac{\int_{t=0}^{t_{end}} \dot{Q}_{sh} \, dt}{W_{el,hp}} \tag{11}$$

Compressor starts

Due to poor control parameter settings, heat pumps in the field can have many compressor starts, resulting in reduced efficiency. Additionally, compressor manufacturers specify a maximum number of starts to ensure a long service life. For this reason, we evaluate the amount of compressor starts for all use cases.

3. Results

This section presents the dynamic simulation results for the three control approaches (section 3.1) and the experimental comparison between both interfaces (section 3.2).

3.1. Simulation case study: MPC vs. heating curve

Figure 5 shows the benchmark case. The black lines show the upper and lower comfort bounds. Between 8 am and 4 pm, they are between 19 °C and 21 °C, else temperatures between 16 °C and 24 °C are within the bounds. For a reasonable comparison with the MPC approaches, the room temperature of the heating curve is set to 16 °C the night. The control of the volume flow behaves accordingly. We get similar room temperature trends in MPC and heating curve control.

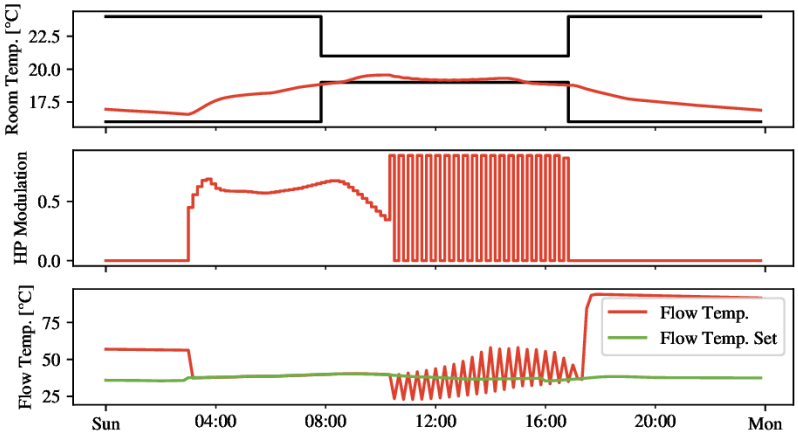

Figure 5: Simulation: Heating the thermal zone on a winter day using a heating curve

It can be seen that the heating curve with the chosen setting can keep the room temperature within the given bounds. The heat pump turns on at around 3:00 am. The heat pump turns on and off frequently as the outdoor temperature rises. The heat pump turns off by lowering the temperature bounds at 4 pm. Since the additional control valve stops the volume flow into the underfloor heating system during low set temperatures, the heat pump can only control the flow temperature during heating hours (3 am – 4 pm; see Figure 4).

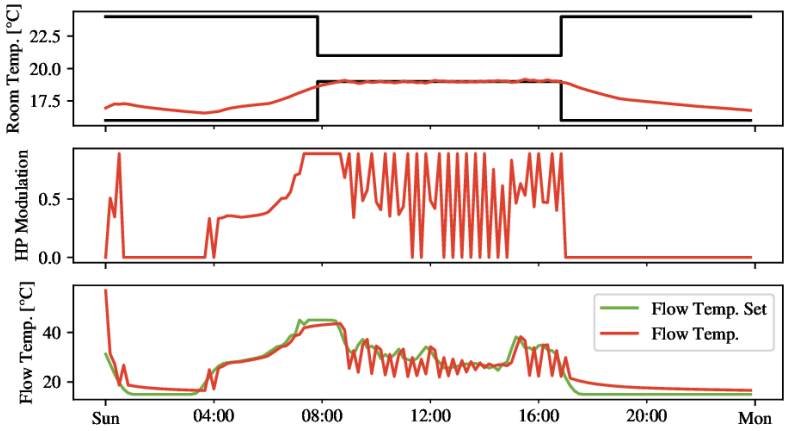

Figure 6: Simulation: Heating the thermal zone on a winter day using an MPC, which controls the flow temperature setpoint.

In Figure 6, the room temperature of the thermal zone is controlled with an MPC that sets the flow temperature setpoint. An internal PID-Controller of the heat pump controls the flow temperature. The MPC can keep the zone temperature within the comfort constraints. To reach the raised bounds at 8 o'clock, the MPC raises the flow temperature setpoint to its upper bound. Between 8 am and 4 pm, a discrepancy between the set and the actual flow temperature is observed. The difference results from frequent on-off cycling of the heat pump caused by the internal PID-Controller. The MPC lowers the flow temperature setpoint by lowering the temperature bounds.

Figure 7 shows the control of the zone temperature with an MPC that directly controls the compressor speed. The MPC is capable of keeping the zone temperature within the comfort constraints. The heat pump gets turned on at around 5 am. Before raising the temperature bounds, the MPC sets the compressor speed to its upper bound to fulfill the temperature bounds. Similar to the MPC with the flow temperature setpoint, the MPC lowers the set value during the day to minimize energy consumption. The discrepancy between the set and the actual heat pump modulation can be explained by the minimum compressor speed of 30 Hz. The compressor gets turned off if the MPC set value is below 30 Hz. Since the relative compressor speed can only

be between 0.33 and 1 and the set value range is between 0 and 1, the compressor can only follow the set fellow from 0.33 to 1.

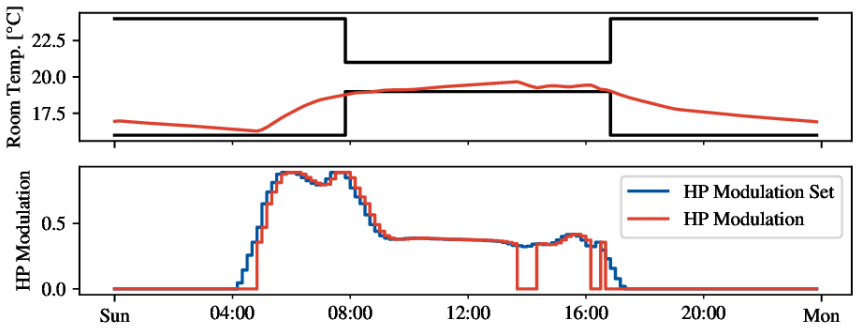

Figure 7: Simulation: Heating the thermal zone on a winter day using an MPC which controls the compressor speed.

Table 1 shows the KPI evaluation of the three simulated control approaches. The consumed electrical energy is 29.38 kWh for the heating curve controller, which is the highest overall value. Both MPC approaches reduce electrical energy consumption. Controlling the flow temperature reduces the energy consumption by 20.25 %, and controlling the compressor speed directly reduces the energy consumption by 5.75 %. The highest discomfort of all control approaches is at 0.32 Kh with the MPC with flow temperature setpoint. The discomfort corresponds to a deviation of the temperature bounds of 0.32 K for one hour, which is negligible for the comfort of occupants.

The heat pump operates the most efficiently with the flow temperature MPC at a SCOP of 2.83. The heating curve controller achieves the lowest SCOP of 2.46. The number of starts for heating curve control and flow temperature MPC is 22 and 24, respectively. Both controllers yield a higher number of starts than compressor speed MPC, which is at 3. Summing up, directly controlling the compressor speed leads to fewer starts. Many compressor starts reduce the service life, but this study cannot measure it. According to the following case study, the heat pump's efficiency needs to be evaluated in real experiments.

Table 1: Simulation: KPI's of the three different control approaches.

Controller	Energy[kWh]	Discomfort[Kh]	SCOP[]	Starts[]
Heating Curve	29.38	0.28	2.46	22
MPC with flow temperature setpoint	23.43	0.32	2.83	24
MPC with compressor speed setpoint	27.69	0.06	2.61	3

3.2. Experimental case study: Integrating MPC into a real heat pump controller

This section demonstrates the successful integration of MPC on a real heat pump system. Figure 8 shows the MPC with flow temperature control. The heat pump first gets turned on at around 4 am, similar to the MPC, which controls the compressor speed. Due to the MPC raising of the flow temperature setpoint, the compressor speed rises until it operates at maximum speed.

With lowering the flow temperature setpoint, we observe several compressor starts between 9 am and 5 pm due to the internal PI controller, which turns off the heat pump if its output is below 0.33. On-off cycling happens if the flow temperature setpoint is too low to be kept with minimum compressor speed. The PI-controller turns off the heat pump, the flow temperature drops below the setpoint, and after the minimum off-time, the heat pump will be turned on again.

Table 2 shows the evaluated KPIs for the experiments with the real heat pump for the two MPC approaches. The electrical energy consumed is 8.15 % lower for the MPC with flow temperature control. The thermal discomfort for this approach is 3.77 Kh and 0.2 Kh for the compressor speed MPC. Table 2 gives an overview of these KPIs. The SCOP is similar to both approaches. Due to the behavior of the internal PI-controller, the flow temperature MPC has 18 starts. With direct control of the compressor speed, the starts are reduced to 2.

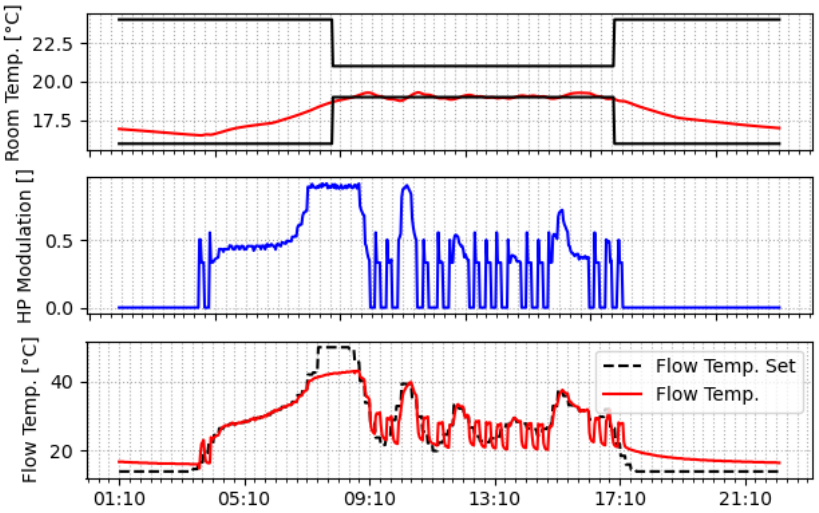

Figure 8: Real experiment: Heating of the thermal zone on a winter day using an MPC, which controls the flow temperature

Figure 9 shows the experimental results of the real heat pump using MPC controlling the compressor speed. The zone temperature and MPC setpoint curves are very similar to the simulated data in Figure 7. The heat pump's compressor can keep the setpoints given by the MPC. Like in the simulations, the heat pump gets turned off at compressor speeds below 30 Hz, corresponding to an MPC setpoint of 0.33.

When the heat pump gets turned on, seen at around 4 am and 11 am, the compressor speed jumps. This starting behavior is given by the prescribed compressor startup program of the compressor's manufacturer. This mode guarantees a safe operation within the highly dynamic starting procedure. After the dynamic starting mode, the heat pump switches to normal mode and accepts set values for compressor speed from the MPC. Staring procedures of heat pumps show real-world limitations, are challenging to model, and underline the importance of dynamic experimental tests. The following section discusses the explained results.

Table 2: Real experiment: KPIs of the three different control approaches.

Controller	Energy[kWh]	Discomfort[Kh]	SCOP[]	Starts[]
MPC with flow temperature setpoint	26.26	3.77	2.69	18
MPC with compressor speed setpoint	28.59	0.2	2.61	2

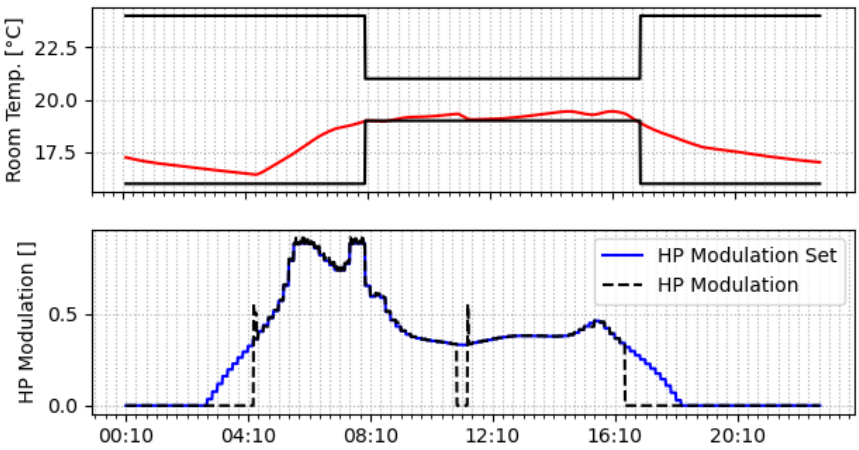

Figure 9: Real experiment: Heating of the thermal zone on a winter day using an MPC, which controls the compressor speed

4. Discussion

In this section, we discuss the results from Section 3 in the context of the identified research gaps. The results show that the simulation and experimental studies provide reasonable results.

The first identified research gap concerns the high implementation effort for MPC. The data-driven MPC method chosen reduces the modeling effort. The results show that the modeling accuracy is sufficient. In the simulative and experimental case studies, the MPC controllers outperform the heating curve controller in energy consumption. The development of the process models requires either field test or simulative data but no physical equations. This work contributes to integrating MPC into practice by overcoming the need for reduced model development effort.

The literature did not investigate the potential of different system controller interfaces on the heat pump system. The results of this work prove the influence of available interfaces on the overall system performance. When comparing the results from Table 2, it is noticeable that the MPC with direct access to the compressor speed leads to lower discomfort (0.2 Kh to 3.8 Kh). If the set flow temperature is manipulated, the heat pump's internal controller calculates the control signal for the compressor. The control signal leads to high inaccuracies that the MPC cannot predict. In addition, the pre-setting of the flow temperature at low modulation increases the number of compressor starts (see Figure 8). As a result, the MPC with flow temperature pre-setting maintains the room setpoint temperature less accurately. If the MPC can control the compressor directly, the number of starts is reduced enormously (from 18 to 2).

One difference between the MPC's setpoint and the heat pump's conversion remains if the modulation setpoint is below 0.33 because the heat pump cannot convert frequencies lower than 30 Hz. Direct compressor control leads to improved comfort and efficient operation with fewer on/off cycles. However, the heat pumps' SCOP does not derivate much between the interfaces. The differences are due to many compressor starts that reduce the average flow temperature. A low flow temperature leads thermodynamically to higher efficiency. Starting processes worsen the efficiency since additional losses occur during the compressor start (high overheating, high friction losses in the compressor). Both effects seem to balance each other out in the investigated experimental case study and should be investigated in more detail in the future.

Finally, purely annual simulative studies usually use simplified models to reduce computational effort. In the simulative case study, the calibrated model accurately describes the steady-state heat pump process. However, the differences between the experiment and simulation, especially in the discomfort, deviate strongly from each other. The differences are not due to MPC computing but due to differences in experimental and simulative heat pump operation. The influence of the compressor starts on the efficiency, and the flow temperature can hardly be represented by a simulation model. Therefore, the experimental data show the real-life behavior and the accurate system technology's influence. The HiL approach, with its dynamic, realistic, and repeatable boundary conditions, contributes to the integration of MPC into the practice.

5. Conclusion

This work contributes to integrating MPC with data-driven process models into practice using simulative and experimental case studies. In this paper, we apply the hardware-in-loop method to prove the functionality of MPC under dynamic, repeatable boundary conditions. We integrate a system controller into an energy system consisting of a self-developed heat pump test bench and a building performance simulation model coupled via a hydraulic test bench and a climate chamber. A conventional heating curve controller represents the benchmark control. The MPC controls the supply temperature or the heat pump's compressor speed exploiting the potential of different controller interfaces. We show that data-driven MPC controllers reduce the modeling effort and still lead to reasonable results outperforming conventional heat pump controller. In all case studies, the MPC reduces the system's energy consumption by up to 20.25 %. Direct access to the compressor frequency reduces the number of startups at from 18 to 2 for one specific day. The reduction of starts leads to a higher control quality and, thus, to low discomfort.

The BES consists only of a heat pump and building in this work. We will extend the system with a DHW tank and PV-System in future work.

Acknowledgments

We gratefully acknowledge the financial support by the German Federal Ministry for Economic Affairs and Climate Action (BMWK), promotional reference 03EN1022B.

References

[1] P.R. Shukla, J. Skea, R. Slade, A. Al Khourdajie, R. van Diemen, D. McCollum, M. Pathak, S. Some, P. Vyas, R. Fradera, M. Belkacemi, A. Hasija, G. Lisboa, S. Luz, J. Malley, 'IPCC, 2022: Climate Change 2022: Mitigation of Climate Change. Contribution of Working Group III to the Sixth Assessment Report of the Intergovernmental Panel on Climate Change'.

[2] IEA, 'Buildings'. 2022. [Online]. Available: https://www.iea.org/reports/buildings

[3] L. Pérez-Lombard, J. Ortiz, and C. Pout, 'A review on buildings energy consumption information', *Energy and Buildings*, vol. 40, no. 3, pp. 394–398, Jan. 2008, doi: 10.1016/j.enbuild.2007.03.007.

[4] J. Drgoňa *et al.*, 'All you need to know about model predictive control for buildings', *Annual Reviews in Control*, Sep. 2020, doi: 10.1016/j.arcontrol.2020.09.001.

[5] G. Serale, M. Fiorentini, A. Capozzoli, D. Bernadini, and A. Bemporad, 'Model Predictive Control (MPC) for Enhancing Building and HVAC System Energy Efficiency: Problem Formulation, Applications and Opportunities', *energies*, Mar. 2018, [Online]. Available: file://eonakku/home/ebc/ses-tsp/Downloads/energies-11-00631-v2.pdf

[6] D. Fischer, J. Bernhardt, H. Madani, and C. Wittwer, 'Comparison of control approaches for variable speed air source heat pumps considering time variable electricity prices and PV', *Applied Energy*, vol. 204, pp. 93–105, Oct. 2017, doi: 10.1016/j.apenergy.2017.06.110.

[7] P. Stoffel, L. Maier, A. Kümpel, T. Schreiber, and D. Müller, 'Evaluation of Advanced Control Strategies for Building Energy Systems', Social Science Research Network, Rochester, NY, SSRN Scholarly Paper 4251878, Oct. 2022. Accessed: Oct. 23, 2022. [Online]. Available: https://papers.ssrn.com/abstract=4251878

[8] T. Pean, R. Costa-Castello, E. Fuentes, and J. Salom, 'Experimental Testing of Variable Speed Heat Pump Control Strategies for Enhancing Energy Flexibility in Buildings', *IEEE Access*, vol. 7, pp. 37071–37087, 2019, doi: 10.1109/ACCESS.2019.2903084.

[9] S. Göbel, T. Fiedler, J. Klingebiel, C. Vering, and D. Müller, 'Development and experimental validation of model-based superheat control strategies for air-to-water heat pumps.' International Institute of Refrigeration (IIR). doi: 10.18462/IIR.GL2022.0143.

[10] F. Wüllhorst, L. Maier, D. Jansen, and D. Hering, 'BESMod - A Modelica Library providing Building Energy System Modules', presented at the American Modelica Conference, Dallas, Texas, 2022.

[11] P. Remmen, M. Lauster, M. Mans, M. Fuchs, T. Osterhage, and D. Müller, 'TEASER: an open tool for urban energy modelling of building stocks', *Journal of Building Performance Simulation*, vol. 11, no. 1, Art. no. 1, Jan. 2018, doi: 10.1080/19401493.2017.1283539.

[12] InfluxData, *InfluxDB key concepts | InfluxData Documentation*. 2023. [Online].

[13] A. Stanford-Clark and A. Nipper, 'Message Queuing Telemetry Transport (MQTT)'. [Online]. Available: http://mqtt.org/

[14] Joel A. E. Andersson, Joris Gillis, Greg Horn, James B. Rawlings, and Moritz Diehl, 'CasADi: a software framework for nonlinear optimization and optimal control', *Math. Prog. Comp.*, no. 11, 2019, doi: https://doi.org/10.1007/s12532-018-0139-4.

[15] A. Wächter and L. T. Biegler, 'On the implementation of an interior-point filter line-search algorithm for large-scale nonlinear programming', *Math. Program.*, vol. 106, no. 1, pp. 25–57, Mar. 2006, doi: 10.1007/s10107-004-0559-y.

[16] J. A. E. Andersson, J. Gillis, G. Horn, J. B. Rawlings, and M. Diehl, 'CasADi: a software framework for nonlinear optimization and optimal control', *Math. Prog. Comp.*, vol. 11, no. 1, pp. 1–36, Mar. 2019, doi: 10.1007/s12532-018-0139-4.

[17] P. Stoffel, C. Loffler, S. Eser, A. Kumpel, and D. Muller, 'Combining Data-driven and Physics-based Process Models for Hybrid Model Predictive Control of Building Energy Systems', in *2022 30th Mediterranean Conference on Control and Automation (MED)*, Vouliagmeni, Greece, Jun. 2022, pp. 121–126. doi: 10.1109/MED54222.2022.9837277.

[18] J. Christoffer, T. Deutschländer, and M. Webs, *Testreferenzjahre von Deutschland für mittlere und extreme Witterungsverhältnisse TRY*. Offenbach: Selbstverlag Deutscher Wetterdienst, 2004.

[19] S. Ioffe and C. Szegedy, 'Batch Normalization: Accelerating Deep Network Training by Reducing Internal Covariate Shift'. arXiv, Mar. 02, 2015. Accessed: Nov. 15, 2022. [Online]. Available: http://arxiv.org/abs/1502.03167

[20] S. Göbel, C. Vering, and D. Müller, 'Experimental Investigation of Rule-Based Control Strategies for Hybrid Heat Pump Systems Using the Smart Grid Ready Interface', in *PROCEEDINGS OF ECOS 2022*, Kopenhagen, 2022.